

Analysis of a wooden specimen's mechanical properties through acoustic measurements in the very near field

.....
Filip Pantelić,^{1,a)} Miomir Mijić,² Dragana Šumarac Pavlović,² Daniel Ridley-Ellis,³
and Danica Dudes¹

¹*School of Electrical and Computer Engineering of Applied Studies, Vojvode Stepe Street 283, Belgrade 11000, Serbia*

²*School of Electrical Engineering, University of Belgrade, Bulevar Kralja Aleksandra 73, Belgrade 11000, Serbia*

³*Centre for Wood Science and Technology, Edinburgh Napier University, Edinburgh, United Kingdom
filip_pantelic@yahoo.com, emijic@etf.rs, dsumarac@etf.rs, d.ridley-ellis@napier.ac.uk, danica.dudes@gmail.com*

Abstract: This paper presents the method for prediction of some basic mechanical parameters of a wood specimen by using simple instrumentation. The standard acoustic method for assessment of modulus of elasticity using the impulse excitation is extended by using a recording in the very near field. In this way, visualization of vibration patterns of the analyzed sample was accomplished for all modes below 5 kHz. This enables detection of signals with a good signal-to-noise ratio over a wide frequency range which is then used for loss factor assessment. © 2020 Acoustical Society of America

[Editor: Greg McDaniel]

Pages: EL320–EL325

Received: 13 January 2020 Accepted: 19 March 2020 Published Online: 9 April 2020

1. Introduction

It is a common technique to assess the modulus of elasticity (MOE) of many materials, based on the acoustic resonance of the sample.^{1,2} For this, it is a common standard procedure to calculate MOE based on the frequency of the first oscillation mode for the flexural waves. In this study, the sample is excited by impulse and the response is measured in the very near field (VNF). The sample must be in free-free boundary conditions, which was achieved by placing it on a pair of elastic bands. According to the above-mentioned standard, the sample must have such dimensions that its length is at least one order higher than the width and thickness. This condition ensures that the first mode of oscillation, for flexure waves along the length of the sample, is at a frequency that is significantly lower than the modes that can occur for other dimensions. In this way, the lowest oscillation mode which occurs in the sample response spectrum can be reliably identified as the first oscillation mode for the flexural waves. The standard application of this procedure is strictly only suitable for materials that are homogeneous and isotropic, which is not the case with wood.

Wood as a material, due to its structure, has different values of MOE for different directions of sample orientation.³ Because of this, a small piece of wood is a typical example of orthotropic material, in which the MOE differs for the directions of the three orthogonal local axes corresponding to the direction of the wood grain. Thus, there are tangential, radial, and longitudinal MOEs. For natural wood the values of the MOE differ significantly for the different orientation directions. In addition to this, the shear moduli for wood are relatively low and typically on the order of 1/16th of the MOEs. In the case of wood that is used to create instruments, the differences in the values of the MOE for different directions can be very large. For the spruce that is used for guitars, MOE in the longitudinal direction could be 13.6 GPa while in the radial direction it can be only 0.24 GPa. According to the literature, for string instruments wood, values could be 16 and 0.5 GPa for the longitudinal and radial direction, respectively.

The velocity of flexural waves in a beam is given by Eq. (1),⁴

$$v = \frac{\sqrt{2\pi f}}{\sqrt[4]{12}} \sqrt[4]{\frac{E}{\rho}} \sqrt{l_y}, \quad (1)$$

where f is frequency, E is the MOE, ρ is the density of material, and l_y is the thickness of the material.

^{a)} Author to whom correspondence should be addressed.

Based on the value of the elastic modulus for different wood orientation, the velocity of flexural waves can be up to 7.5 times higher in the longitudinal direction than in the radial direction. Due to the lower wave velocity in the radial direction in the sample, standing waves that occur along this axis tend to have lower frequencies. For this reason, when wood characteristics for the longitudinal direction are to be estimated, a more rigorous condition is needed for the proportions of the analyzed sample. When the sample has to be analyzed for the radial direction, its longest dimension must follow this orientation. It is then ensured that the lowest mode of flexural waves occur in the radial direction, even for a smaller ratio of length and width than that indicated in the standardized procedure.

Due to these properties of wood, for someone with no experience in recognizing the internal structure of the wood, there is uncertainty in identifying the desired oscillation mode. Indeed, even when the grain directions are known, there can still be numerous frequencies present for modes that are hard to identify. In the frequency spectrum of the analyzed response signal there is also sometimes another low resonance of the system which is a consequence of an entire sample oscillating on its supports. For this reason, it is good to also identify higher modes of the system based on the ratio between their frequencies and the frequency of the first mode in order to unambiguously determine the first oscillation mode for the flexural waves.

What is most likely to contribute to identification is the visualization of these modes. Visualization can be performed by various optical methods, such as optical holography or laser Doppler vibrometry.⁵⁻⁸ A simple method that proved to be good for this purpose without the need for special equipment, and which is presented in this paper, is the scanning of a sample in the VNF.⁹⁻¹¹

It is possible to visualize the modes of vibration by VNF measured in a large number of positions alongside the sample. Using this technique, visualization and identification of modes can be achieved so it is also possible to calculate the MOE according to higher order modes. Visualization is particularly important when examining a material in which the value of MOE cannot be reliably predicted, or if, due to the geometry of the sample around the first flexural mode, there is another mode (e.g., torsional) with which it can be mixed with.

If the sound is registered with a microphone in the VNF, approaching the vibrating surface at only 3 mm, the repeatability of such measurements will increase. Contrary to this, to do near-field measurements means small changes in the position of the microphone result in large differences in the recorded response. In the VNF the pressure above the observed surface is directly proportional to the local velocity of the vibrating surface.¹²

The dynamic MOE for flexural vibration is commonly calculated by a theoretically derived expression similar to Eq. (2),

$$E = \rho \left[\frac{2\pi\sqrt{12}f_n l_x^2}{C_n^2 l_y} \right]^2, \quad (2)$$

where E is MOE, f_n are frequencies at which modes occur, l_x is the length of the sample, l_y is the sample thickness, ρ is the sample density, C_n are the coefficients that depend on the boundary conditions of the analyzed (Euler–Bernoulli) beam. For free-free boundary conditions these are solutions of the condition $\cos(C) = 1/\cosh(C)$. For the first five modes those coefficients are: $C_1 = 4.7300$, $C_2 = 7.8532$, $C_3 = 10.9956$, $C_4 = 14.1372$, $C_5 = 17.2788$ (Refs. 13 and 14). For higher modes ($n \geq 5$) these shape function coefficients can be obtained using the widely used approximation, Eq. (3). Reference 15 lists equations for other boundary conditions and the theoretical background.

$$C_n = n\pi + \frac{\pi}{2}. \quad (3)$$

This theoretical Eq. (2) is, however, based on assumptions that do not hold well for wood. The difference is the contribution of shear to the flexural vibration, which becomes more significant as the beam becomes relatively deeper compared to the wavelength (i.e., for higher modes). Most theoretical equations that do include shear do so assuming the shear modulus (G) is simply related to MOE by the Poisson's ratio, as is the case for isotropic materials. For wood, the role of G in flexural vibration needs to be considered explicitly when higher order modes are inspected. This is much more complicated than the normally applied equation, but a relatively simple formulation of this, and an approach to solution, has been provided by Ref. 16 in the wood science literature. A further advantage of this is that, if the identification of oscillation modes is successfully performed, it is also possible to estimate the MOE using frequencies of higher order modes, and by doing so also estimate G .

Loss factor η can be used in material testing or in evaluating a composite structure. It directly measures dissipation, with no reference to the physical mechanisms involved.¹⁷ The total losses are the sum of internal losses, radiation losses, and boundary losses. Different damping mechanisms operate at different frequency ranges. Radiation losses are particularly relevant in the coincidence region.¹⁸ It is the frequency region starting from frequency where the wavelength of sound in air is the same as the wavelength of flexural waves at the radiating surface.¹⁹ Radiation losses are significant when measuring small loss factors ($\eta < 10^{-4}$). In the case of wood, the usual values of a loss factor are higher. If all other losses are discarded and only losses due to heat conduction are considered then the model predicts that the curve of a loss factor increases with frequency in the normal audio frequency region.²⁰ For bending vibrations the regions of different temperatures are very close to each other. For a beam or a plate, the upper side, for instance, heated and compressed, and the lower side, extended and cooled, are at a distance equal to the thickness of the beam or the plate. For bending vibrations, the value of the loss factor may then be higher and at the same time may rise more quickly as a function of frequency than for the case of longitudinal vibrations.

The phase difference of stress and strain implies that mechanical energy is lost.²¹ Loss factor could be measured directly by measuring phase difference between the force and displacement. In this way accuracy of about 0.2° is needed for measuring loss factors on the order of $\eta \sim 10^{-4}$. Usually loss factor is measured indirectly. The estimation of the loss factor can be made by using the logarithmic decrement of the time form of these signals or from the Q -factor obtained from the frequency spectrum of the impulse response.³ Experimental methods such as the 3 dB method used for materials and structures actually evaluate modal damping in the form of a figure of merit. With these methods, calculation of spectrum is required. The usual form $\eta = 1/Q$ is correct, within an error less than 1%, if $0 \leq \eta \leq 0.28$. For very small damping, more accurate results can be obtained by measuring decay (or reverberation) times than by measuring half-value bandwidths, but different methods in signal processing can be used to improve this method, e.g., Ref. 22.

When measuring loss factor by measuring the structural reverberation time formula

$$\eta = \frac{2.2}{fT_{30}}, \tag{4}$$

is used by many authors^{18,23} where T_{30} is reverberation time and f is the central frequency of a 1/3 octave band. In these cases, multiple modes appear within the observed interval, so the phenomenon of energy decay is observed integrally for that frequency range. A similar concept is also used in this paper, with the exception that each mode of the analyzed beam is filtered in a very narrow band, so that signals do not contain other modes. For this reason, f is the exact value of the oscillating frequencies. The same procedure was performed for each individual mode calculating the reverberation time by using the Schroeder's curve which is obtained by the backward integration of a squared impulse response.

2. Measurement

2.1 Experimental setup

The estimation of the MOE that is presented in this paper refers to the dynamic MOE in the longitudinal direction. The internal structure of the analyzed sample is oriented to ensure that the longest dimension of the sample matches the longitudinal direction of the wood grain, which is shown in Fig. 1 (left). Wood density is not uniform but in this procedure it is assumed that the mass is evenly distributed throughout the volume of the sample. This is a reasonable assumption when the growth rings are relatively small compared to the sample dimensions. The dimensions of the analyzed sample were length $l_x = 0.456$ m, thickness $l_y = 0.0035$ m, and width $l_z = 0.0198$ m, while the mass was $m = 0.02346$ kg. In this case, the length is 23 times higher than the width, which indicates that the lowest oscillation mode occurs along the length of the sample.

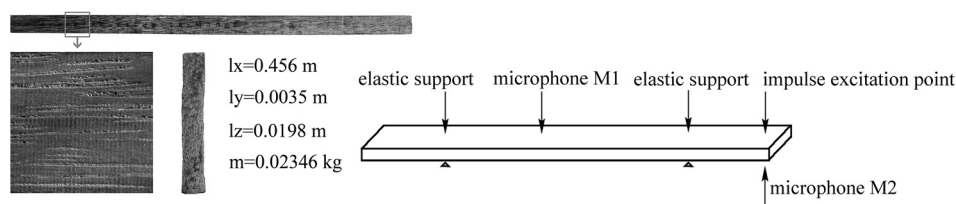


Fig. 1. Characteristics of the sample which is used in the experiment (whole sample, detail and cross section) (left); experimental setup (right).

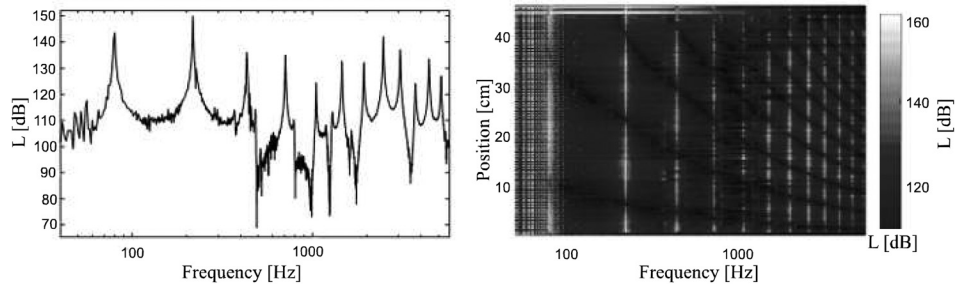


Fig. 2. Impulse response spectrum (left); visualisation of vibration modes by scanning the sample in VNF. Light tones: maximums; dark tones, minima, i.e., the nodes of standing waves (right).

The experimental setup is shown in Fig. 1 (right). The sample is placed on elastic bands in order to achieve free-free boundary conditions. During the measurement, the specimen was manually excited by impulse (hammer) consistently at the same point. In addition to the sample on elastic bands, this setup employs two ordinary consumer microphones with 10 mm membrane diameter. The moveable microphone, M1, is set in a VNF, at a distance of several millimeters from the sample. The microphone progressively recorded response at 92 points along the length of the sample. The non-uniformity of the sample excitation for each measurement point is compensated by the referent microphone M2. This microphone is positioned in VNF at one set point, and it does not move through all measurements. Its role is to register variations in different levels of sound pressure due to a non-uniform hammer impact. The signals recorded with the M1 microphone are increased or decreased according to variations of signal level recorded with the M2 microphone.

2.2 MOE

The spectrum of one impulse response, measured in a VNF at one point above the oscillating sample, is shown in Fig. 2 (left). From this graph frequencies at which the modes appear can be read. These frequencies are shown in Table 1. At about 19 Hz in the frequency spectrum there is resonance as a consequence of the entire sample oscillating on the elastic band supports, and since this is irrelevant to the wood properties it is not considered in further analysis.

Impulse response was recorded at 92 measuring points that were evenly distributed along the sample. For each recorded signal a spectrum with a frequency resolution of 1 Hz in the frequency range 1 to 22 050 Hz was calculated (this frequency range corresponding to ordinary consumer audio equipment). The calculated spectra for the 92 points are placed in a $92 \times 22\,050$ matrix. The graphical representation of this matrix is shown in Fig. 2 (right). This graph represents the dependence of the sound pressure level from the frequency and from the position of measurement. In the VNF sound pressure is proportional to the surface velocity at the local point above which the microphone is placed, so this graph elucidates the oscillation modes of the analyzed wooden beam. The bright tones show the maximums, while the black ones represent minima, i.e., the nodes and antinodes of the standing waves that occur across the sample.

Resonances in the spectrum of Fig. 2 (left) can be identified from these patterns appearing in Fig. 2. (right). According to Eq. (2), the values of the MOE based on these frequencies can be calculated. The estimated values are also shown in Table 1. The values of the MOE, which apparently depend on the frequency at which it is estimated, are shown in Fig. 3. The

Table 1. Specimen resonant frequencies, MOE, and loss factor.

Mode No.	1	2	3	4	5	6	7	8	9	10
f [Hz]	79	217	425	700	1036	1451	1912	2447	3038	3684
Eq. (2) Apparent E_y [GPa]	15.46	15.35	15.32	15.21	14.93	15.02	14.71	14.6	14.43	14.21
Ref. 16 E_y [GPa]						15.51				
G [GPa]						0.932				
f calculated [Hz]	79	217	425	699	1040	1444	1909	2433	3040	3713
error	0.00%	0.00%	0.00%	-0.10%	0.40%	-0.50%	-0.20%	-0.60%	0.10%	0.80%
T_{30} [s]	5.65	2.16	1.12	0.67	0.38	0.26	0.18	0.14	0.11	0.07
η	0.0050	0.0047	0.0046	0.0046	0.0055	0.0058	0.0064	0.0063	0.0065	0.0084

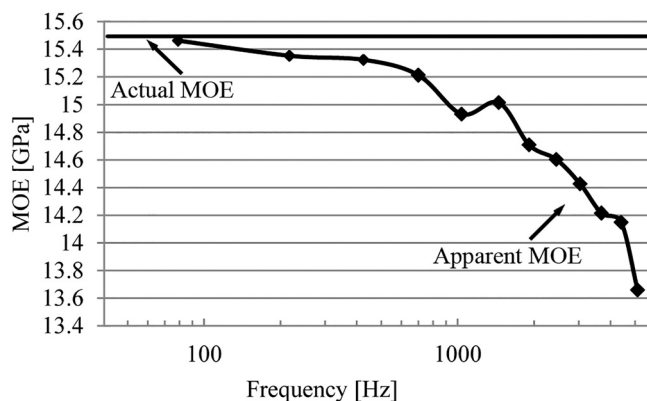


Fig. 3. Dependence of MOE approximation on frequency.

stiffness of wood is dependent on the rate of loading, but this apparent drop in MOE with frequency is actually an error, caused by the unsuitability of Eq. (2) for wood, and the increasing involvement of G in the flexural vibration. When the method of Ref. 16 is applied instead, the frequencies can be matched well by a single combination of MOE and G (15.51 and 0.931 GPa, respectively). These are quite typical values for wood.

2.3 Loss factor

The loss factor determines how long the sample will oscillate after the excitement. The levels of the signals of some harmonics can be quite low, so in some cases it is difficult to reach the value of the reverberation time T_{30} . As these harmonics quickly disappear, it is possible to make a useful recording only in the VNF. Positions where the desired harmonic has the highest level could be identified from Fig. 2 (right). Taking the signal from that position, it is possible to determine its reverberation time and estimate the loss factor. That kind of signal selection provides a good signal-to-noise ratio. Figure 4 (left) shows Schroeder's curve for the tenth oscillation mode that occurs at a frequency of 3684 Hz, which has a constant slope for almost 60 dB. Using the Schroeder's curve reverberation time T_{30} is calculated in the frequency bands of all identified modes. From those data, using Eq. (4), values of the loss factor for the analyzed ranges can be obtained. The values of the loss factor for these modes are also shown in Table 1.

Figure 4 (right) shows the dependence of the estimated value of the loss factor from the frequency. The loss factor values are quite uniform in the observed frequency band. The usual values for this parameter for wood are from 0.01 to 0.1.²⁰ In the case of the analyzed sample, the estimated value tends to reach a lower limit of this range: this specimen has a low damping factor. Since the attenuation coefficients have low values, the resonances of the damped vibrations of this sample f , which are read from the spectrum shown in Fig. 2, and defined by Eq. (5),²⁴ slightly deviate from the case of undamped vibration resonance f_n for which Eq. (2) and the method of Ref. 16 is defined.

$$f = \sqrt{f_n^2 - (\pi\eta f_n)^2}. \tag{5}$$

For this reason, in this particular case losses do not affect the estimated value of the MOE. When the loss factor is equal to $\eta=0.01$, the differences in the resonant frequencies of damped and undamped vibrations are less than 0.1%. For a wood sample with a large loss factor

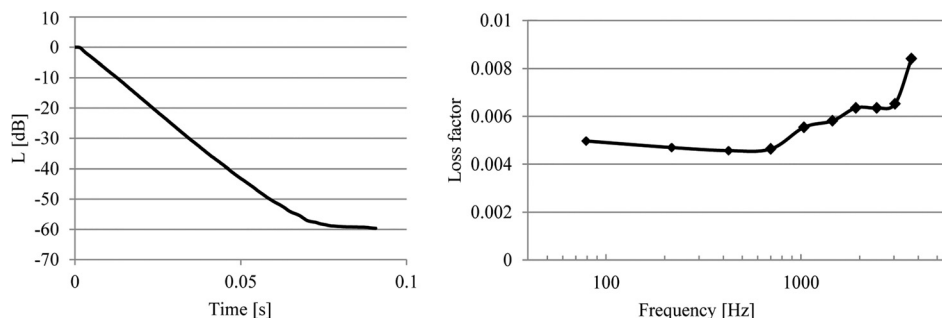


Fig. 4. Schroeder's curve for the tenth vibration mode (left); dependence of loss factor approximation on frequency (right).

($\eta = 0.1$) the value of the resonant frequency of damped vibrations is 5% less than the value of the resonant frequency of undamped vibrations. For this reason, when analyzing the sample with a large loss factor, this variation must be taken into account when evaluating the MOE.

3. Conclusion

The method used has proved to be suitable for the analysis of the stiffness properties of wood without the need for specialist equipment. The measurement method in a VNF allows good visualization of vibration patterns for frequencies up to 5 kHz which makes possible the identification of oscillation modes and thus eliminates some doubts when evaluating the MOE. Visualization of oscillation modes is also useful in selecting the signals for the loss factor calculation, because the measuring points where the mode of interest has the highest level in the total signal can be determined, which ensures the best signal-to-noise ratio.

As far as radiation losses is concerned, besides being neglected for relatively high wood loss factor values, it can also be neglected based on the radiation efficiency for that particular case and frequency range, which can be concluded from VNF measurement. Based on the wavelengths of the flexural waves that can be read from Fig. 2 (right), the critical frequency of this sample is estimated to be about 4 kHz. Starting from the mode at 4409 Hz the wavelength on the beam, which is 8 cm, becomes longer than the wavelength for that frequency in the air, which is 7.8 cm. Radiation is greater in the frequency region that is out of our scope.

Although the method does not require complicated or expensive instrumentation it gives good results which makes it applicable to a large number of users. It is much more important to apply the more sophisticated theoretical equations for calculation.

References and links

- ¹ASTM E1875-13, "Standard test method for dynamic Young's modulus, shear modulus, and Poisson's ratio by sonic resonance" (ASTM International, West Conshohocken, PA, 2013).
- ²ASTM E1876-15, "Standard test method for dynamic Young's modulus, shear modulus, and Poisson's ratio by impulse excitation of vibration" (ASTM International, West Conshohocken, PA, 2015).
- ³V. Bucur, *Acoustics of Wood* (Springer-Verlag, Berlin, 2006).
- ⁴Y.-H. Kim, *Sound Propagation: An Impedance Based Approach* (John Wiley & Sons, Asia, 2010).
- ⁵E. Jansson, N.-E. Molin, and H. Sundin, "Resonances of a violin body studied by hologram interferometry and acoustic methods," *Phys. Scripta* **2**, 243–256 (1970).
- ⁶G. Bissinger and D. Oliver, "3-D laser vibrometry on legendary old Italian violins," *Sound Vib.* **3**(7), 10–14 (2007).
- ⁷C. Kalkert and J. Kayser, "Laser Doppler velocimetry," Biophysics Laboratory, University of California, San Diego (2010).
- ⁸P. Gren, K. Tatar, J. Granstrom, N.-E. Molin, and E. V. Jansson, "Laser vibrometry measurements of vibration and sound fields of a bowed violin," *Meas. Sci. Technol.* **17**, 635–644 (2006).
- ⁹J. Prezelj, P. Lipar, A. Belšak, and M. Čudina, "On acoustic very near field measurements," *Mech. Syst. Signal Processing* **40**, 194–207 (2013).
- ¹⁰F. Pantelić and J. Prezelj, "Hair tension influence on the vibroacoustic properties of the double bass bow," *J. Acoust. Soc. Am.* **136**(4), EL288–EL294 (2014).
- ¹¹D. E. Keele, "Low-frequency loudspeaker assessment by nearfield sound-pressure measurement," *J. Audio Eng. Soc.* **22**(3), 154–162 (1974).
- ¹²H.-E. de Bree, V. Svetovoy, R. Raangs, and R. Visser, "The very near field, theory, simulations and measurements of sound pressure and particle velocity in the very near field," in *Eleventh International Congress on Sound and Vibration (ICSV-11)*, St. Petersburg, Russia (2004).
- ¹³L. Meirovitch, *Elements of Vibration Analysis* (McGraw-Hill, New York, 1986).
- ¹⁴F. Pantelić, D. Ridley-Ellis, M. Mijić, and D. Šumarac Pavlović, "Monitoring changes in wood properties using Very Near Field sound pressure scanning," in *4th Annual Conference COST FP1302 WoodMusICK*, Brussels, Belgium (October 5–7, 2017).
- ¹⁵P. J. P. Gonçalves, M. J. Brennan, and S. J. Elliott, "Numerical evaluation of high-order modes of vibration in uniform Euler–Bernoulli beams," *J. Sound Vib.* **301**(3–5), 1035–1039 (2007).
- ¹⁶L. Brancheriau, "An alternative solution for the determination of elastic parameters in free–free flexural vibration of a Timoshenko beam," *Wood Sci. Technol.* **48**, 1269–1279 (2014).
- ¹⁷M. Carfagni, E. Lenzi, and M. Pierini, "The loss factor as a measure of mechanical damping," in *Proceedings of the 16th International Modal Analysis Conference* (1998), Vol. 3243, p. 580.
- ¹⁸E. A. Piana, C. Petrogalli, D. Paderno, and U. Carlsson, "Application of the wave propagation approach to sandwich structures: Vibro-acoustic properties of aluminum honeycomb materials," *Appl. Sci.* **8**(1), 45 (2018).
- ¹⁹J. H. Rindel, *Sound Insulation in Buildings* (Taylor & Francis Group, London, 2018).
- ²⁰D. Ouis, "On the frequency dependence of the modulus of elasticity of wood," *Wood Sci. Technol.* **36**, 335–346 (2002).
- ²¹L. Cremer and M. Heckl, *Structure-Borne Sound* (Springer-Verlag, Berlin Heidelberg, 1988).
- ²²D. Ridley-Ellis, M. Libeau, and D. Mignerat, "Impulse excitation measurement of small changes in elastic moduli and damping using R," *Int. Wood Products J.* **9**, 74–79 (2018).
- ²³T. Asakura, T. Ishizuka, T. Miyajima, M. Toyoda, and S. Sakamoto, "Finite-difference time-domain analysis of structure-borne sound using a plate model," *Acoust. Sci. Technol.* **34**(1), 48–51 (2013).
- ²⁴S. Floyd, "Free and forced vibrations of cantilever beams with viscous damping," NASA Technical Note, National Aeronautics and Space Administration, Washington DC (1965).